Adsorption of ochratoxin A (OTA) anodic oxidation product on glassy carbon electrodes in highly acidic reaction media: Its thermodynamic and kinetics characterization

Eduardo Alejandro Ramírez [a], María Alicia Zón [a], Paola Andrea Jara Ulloa [b], Juan Arturo Squella [b], Luis Nuñez Vergara [b], Héctor Fernández [a,*]

[a] *Departamento de Química, Facultad de Ciencias Exactas, Físico-Químicas y Naturales. Universidad Nacional de Río Cuarto, Agencia Postal No. 3, 5800 Río Cuarto, Argentina*
[b] *Laboratorio de Bioelectroquímica, Facultad de Ciencias Químicas y Farmacéuticas, Universidad de Chile, Olivos 1007, Santiago, Chile*

Keywords:
Ochratoxin A
Adsorptive accumulation
Cyclic voltammetry
Square wave voltammetry
Thermodynamic and kinetics parameters

A B S T R A C T

We study the thermodynamics and kinetics of the adsorption of a redox couple having quinone nature on glassy carbon electrodes. This couple is produced by the anodic oxidation of mycotoxin ochratoxin A in 10% acetonitrile + 90% 1 M $HClO_4$ aqueous solution. The quasi-reversible redox couple was studied by both cyclic (CV) and square wave (SWV) voltammetric techniques. The Frumkin adsorption isotherm best described the specific interaction of the redox couple with carbon electrodes. By fitting the experimental data, we obtained values of $-28.4\,kJ\,mol^{-1}$ and 0.70 ± 0.02 for the Gibbs free energy of adsorption and the interaction parameter, respectively. SWV fully characterized the thermodynamics and kinetics of the adsorbed redox couple, using a combination of the "quasi-reversible maximum" and the "splitting of SW peaks" methods. Average values of 0.609 ± 0.003 V and 0.45 ± 0.06 were obtained for the formal potential and the anodic transfer coefficient, respectively. Moreover, a formal rate constant of $10.7\,s^{-1}$ was obtained. SWV was also employed to generate calibration curves. The lowest concentration of mycotoxin was 1.24×10^{-8} M (5 ppb), measured indirectly with a signal to noise ratio of 3:1.

1. Introduction

Ochratoxin A (OTA), or 7-carboxyl-5-chloro-8-hydroxyl-3,4-dihydro-3R-methylisocoumarin-7-L-β-phenylalanine (Fig. 1a), is a colorless crystalline compound that belongs to a group of closely related derivatives of isocoumarin linked to L-phenylalanine and classified as pentaketides [1]. OTA is a secondary metabolite produced by fungi of the *Penicillium* (*e.g. P. verrucosum*) and *Aspergillus* (*e.g. A. ochraceus*) genera. It is a known teratogen and immunosuppressive agent and has been implicated in Balkan nephropathy in humans. The International Agency for Research on Cancer (IARC) lists OTA as possibly carcinogenic to humans (Group 2B) [2]. Humans can consume OTA in vegetal and animal products [3–5]. For this reason, many countries have restricted OTA levels in food, with upper limits of 1 and 10 ppb depending on the type and quality of the foodstuff [3].

With imports and exports of agricultural commodities increasing in recent years, monitoring of OTA is essential for food safety in the world-wide market. Many research groups have been studying methods for monitoring naturally occurring OTA in a number of agricultural commodities [3,6]. Like many other mycotoxins, OTA is primarily detected and quantified using liquid chromatography in conjunction with fluorimetric detectors and by LC–MS techniques [7–10]. Thin-layer chromatography and enzyme-linked immunosorbent assay (ELISA) are alternative methods. Today, the electroanalytical methods are very valuable alternatives to other methods because no separation procedure is required prior to substrate determination. Furthermore, the required instrumentation is typically less expensive, smaller amounts of solvent are necessary and analysis time is shorter for electroanalytical methods over chromatographic measurements.

To secure these advantages, competitive ELISA methods have been proposed for the quantification of OTA. One such direct method uses polyclonal antibodies [11]. Another uses screen-printed electrodes for quantitative determination of OTA [12], with detection limits in the range 0.9 and $100\,\mu g\,l^{-1}$ for the direct and indirect assay format, respectively. Two ELISA strategies were recently investigated for the development of OTA electrochemical immunosensors based on different OTA immobilization procedures. These immunosensors were suitable as screening tools to detect OTA in wine [13]. In addition, a novel electrochemical immunosensor for sensitive detection of OTA based on screen-printed gold electrodes modified with a layer of 4-nitrophenyl diazonium salt was recently reported. A detection limit

* Corresponding author. Tel.: +54 358 467 6440; fax: +54 358 467 6233.
E-mail address: hfernandez@exa.unrc.edu.ar (H. Fernández).

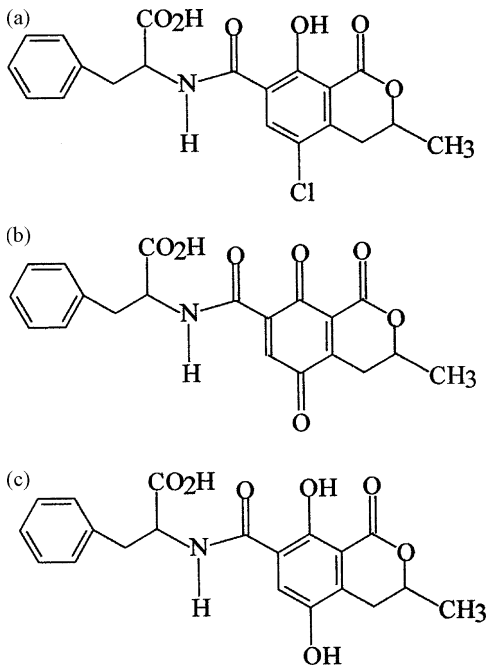

Fig. 1. Chemical structure of: (a) ochratoxin A, (b) OTQ and (c) OTHQ.

of 12 ng ml^{-1} was achieved [14]. Another label-free electrochemical immunosensor developed on modified gold electrodes for sensitive detection of OTA was also recently published [15]. However, fundamental studies on the electrochemical behavior of OTA are necessary to assess the feasibility of employing these electroanalytical methods.

To our knowledge, a few papers presently exist addressing the electrochemical behavior of OTA [16,17]. The electrochemical oxidation of OTA in acetonitrile (ACN) has been reported, as well as that in phosphate aqueous buffer solutions in the pH range from 6 to 8 [16]. A direct correlation with the oxidative behavior of 4-chlorophenol was established. The electrochemical oxidation of OTA in aqueous buffer solutions of different chemical composition in the pH range from 2 to 12 was also recently reported [17]. In this study, we report an adsorbed product of OTA anodic oxidation having quinone nature, which we observed in ACN and in acidic aqueous solutions (OTQ) [16]. Its anodic oxidation voltammetric response depended on pH, but no in-depth investigation of the adsorption characteristics of OTQ was carried out.

In this article, we report the results of our studies on the thermodynamics and kinetics of the adsorption of OTQ on glassy carbon (GC) electrodes in 10% acetonitrile (ACN) + 90% 1 M $HClO_4$ aqueous solution. A surface-based quasi-reversible redox couple was obtained from the adsorption of OTQ, which has been ascribed to an OTA type quinone (OTQ)/hydroquinone (OTHQ) derivative (Fig. 1b and c) [16]. This was characterized by cyclic (CV) and square wave (SWV) voltammetric techniques. Surface charge transfer kinetics and thermodynamic data for the OTQ/OTHQ redox couple were computed by identifying the quasi-reversible maximum and by splitting the square wave voltammetric peaks [18–24]. These results have very promising analytical applications for indirect determination of OTA at trace levels.

2. Experimental

2.1. Reagents

OTA was purchased from SIGMA and used as received. ACN and H_2O were HPLC grade from Sintorgan. $HClO_4$ (Merck p.a.) was used without further purification. Stock solutions of OTA were prepared in ACN and kept at 4 °C in the dark. Working solutions were prepared daily by adding aliquots of stock solution to 10% ACN + 90% aqueous 1 M $HClO_4$. The solution used for OTA spontaneous adsorption was 1.2×10^{-4} M OTA in 10% ACN + 90% aqueous 1 M $HClO_4$. For safety reasons, plastic gloves were used in all manipulations. Most of the experiments were carried out in blank solutions composed of aqueous 1 M $HClO_4$. The influence of pH on the surface redox couple was studied in buffer solutions prepared by combining 0.2 M Na_2HPO_4 (Merck p.a.) with 0.2 M KH_2PO_4 (Merck p.a.). The pH of the solutions ranged from 1 to 12. Solutions were prepared from the above buffer solution and their pH values were adjusted by adding different volumes of 1 M $HClO_4$ or 1 M NaOH.

2.2. Apparatus and experimental measurements

CV and SWV experiments were performed with an AutoLab PGSTAT 12 potentiostat, controlled by GPES 4.9 electrochemical software from Eco-Chemie, Utrecht, The Netherlands. In CV measurements, the scan rate (ν) was varied from 0.005 to 0.100 V s^{-1}. For SWV, a square wave amplitude of ΔE_{SW} = 0.025 V and a staircase step height of ΔE_s = 0.005 V were predominantly used. The frequency (f) was varied from 9 to 40 Hz. In some experiments, ΔE_{SW} was varied from 0.025 to 0.125 V.

Electrochemical measurements were performed in a two-compartment Pyrex cell [25]. The working electrode was a GC disk (BAS, 3 mm diameter). It was polished with 0.3 and then 0.05 μm wet alumina powder (from Fischer), copiously rinsed with water and sonicated in a water bath for 2 min. Then, it was electrochemically activated in aqueous 1 M KOH (Merck p.a.) by applying a potential of 1.2 V over 5 min, according to a methodology described by Anjo et al. [26]. Finally, it was transferred to a blank solution (aqueous 1 M $HClO_4$) and cycled 10 times between 0 and 1.4 V. Anodic and cathodic peak currents ($I_{p,a}$ and $I_{p,c}$), peak potentials ($E_{p,a}$ and $E_{p,c}$) and the difference between anodic and cathodic peak potentials (ΔE_p), were highly reproducible when this pre-treatment was applied to the working electrode. The counter electrode was a large-area platinum foil (approximately 2 cm^2). The reference electrode was an aqueous saturated calomel electrode (SCE) fitted with a fine glass Luggin capillary containing a bridge solution identical to that containing the sample being measured. While no difference was observed in voltammetric responses in aerated *vs.* deareated solutions, to ensure reproducible measurement conditions samples were deareated by bubbling purified nitrogen through the solutions for at least 10 min prior to measurement. The temperature was 20 ± 0.2 °C.

Experimental data were fitted using a nonlinear least squares procedure in Origin 7.0 to determine the adsorption isotherms which best described the specific interaction of OTQ with GC electrodes. The Chi-square function (χ^2) was employed to choose the best fit between experimental and theoretical data.

3. Results and discussion

3.1. Cyclic voltammetry

Cyclic voltammograms of OTA recorded at different pH on activated GC electrodes resembled those in the literature [16,17], and the OTA oxidation peaks ($E_p \approx 1.1$–1.2 V; pH 1) were shifted to less positive potentials with pH ($E_p \approx 0.8$; pH 8–12). These results agree qualitatively with those of Oliveira et al. [17] who worked within a similar pH range (2–12). On reversing the potential sweep no complementary cathodic peak was observed, but another surface-based peak system appeared at less positive potentials for pH < 6. This has been assigned to the reduction/oxidation of an OTA anodic oxi-

dation product, *i.e.*, benzoquinone (OTQ)/hydroquinone (OTHQ) of OTA [16,17], adsorbed onto the GC electrode surface. As the acidity of the medium increased, the reversibility of the peak system also increased, and higher peak currents were obtained. Thus, the rest of the experiments here were conducted in a very acidic medium. Consecutive cyclic voltammograms of OTA in 10% ACN + 90% aqueous 1 M $HClO_4$ are shown in Fig. 2 for the potential range 0 to 1.4 V. A main oxidation peak was observed during the first anodic scan, with a potential peak at about 1.30 V. When the potential sweep was reversed, the complementary cathodic peak was not observed, indicating clearly a complicated reaction mechanism with one or more chemical reactions coupled to the initial electron transfer [16,27]. However, two cathodic peaks were found during the first reversal cathodic scan, centered at potentials about 0.60 and 0.47 V, respectively. A new wide anodic peak, complementary to the cathodic peak at 0.5–0.6 V, was found at a potential of about 0.73 V during the consecutive second anodic scan. Current values for this cathodic and anodic peak system increased with consecutive scans until constant current values were observed after the fifth potential scan. A remarkable decrease of ΔE_p was observed compared with similar results in ACN [16], where a marked solvent effect was observed. Also, better peak definition was achieved here compared with the results of Oliveira et al. [17]. This is due to the relative magnitudes of the peak currents and half-height peak widths for both anodic and cathodic peaks. The differences in results may be attributed to the use of electrochemically activated GC electrodes in this work, compared with the electrodes in Olivieira et al., which were just mechanically polished with alumina. Thus it is clear that the electrochemical and adsorption properties of OTA and its anodic oxidation product (OTQ) are much stronger on activated GC electrodes in a very acidic aqueous medium.

After cycling the working electrode five times in a 10% ACN + 90% aqueous 1 M $HClO_4$ solution containing the mycotoxin, the electrode was copiously rinsed with water and transferred to another electrochemical cell. The new cell either contained the blank solution (aqueous 1 M $HClO_4$) or a buffer solution, with 0.2 M ionic strength and with pH varying from 1 to 10.01. Cyclic voltammograms obtained under these conditions are shown in Fig. 3. A surface-based quasi-reversible peak system was observed, corresponding to oxidation and reduction of the OTHQ/OTQ redox couple. The surface-based nature of the system was confirmed by

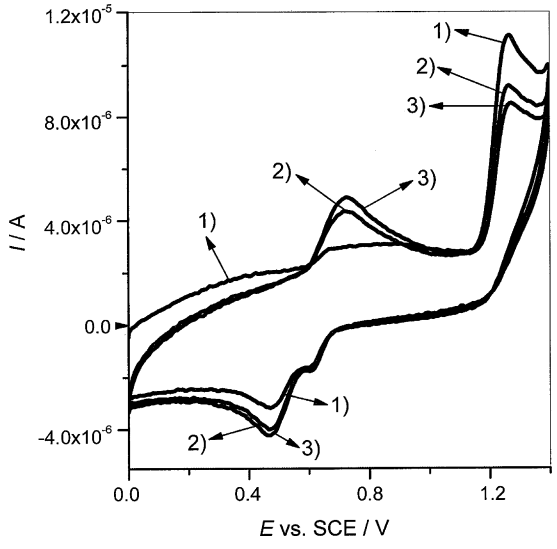

Fig. 2. Cyclic voltammograms of OTA recorded in 10% ACN + 90% 1 M $HClO_4$. Here $c^*_{OTA} = 6.2 \times 10^{-4}$ M, $\nu = 0.050$ V s^{-1}, the working electrode was a GC disk with area $A = 0.0707$ cm^2, and the reference electrode was SCE. (1)–(3) are the first, the third and the tenth potential scan, respectively.

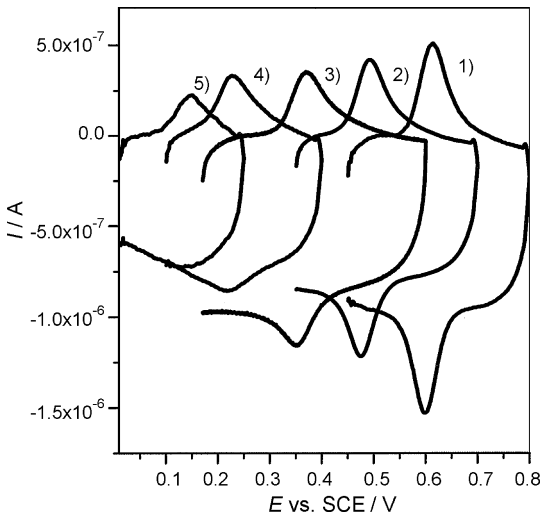

Fig. 3. Cyclic voltammograms of OTHQ adsorbed onto GC electrodes in a 1 M $HClO_4$ aqueous medium (1) and in buffer solutions with pH = 2.95 (2), 4.97 (3), 7.03 (4) and 10.01 (5). OTQ was obtained by cycling the working electrode five times in a solution comprised of 1.24×10^{-4} M OTA in 10% ACN + 90% 1 M $HClO_4$. Here $\nu = 0.025$ V s^{-1}, the working electrode was a GC disk of area $A = 0.0707$ cm^2 and the reference electrode was SCE.

the linear variation of peak currents with sweep rate. For instance, in aqueous 1 M $HClO_4$ solution, a plot of $I_{p,a}$ *vs.* sweep rate (ν) was linear, with a slope of $(47 \pm 3) \times 10^{-6}$ A s V^{-1} and a correlation coefficient of $r = 0.9963$. For solutions with pH values from 1 to 8, cyclic voltammograms were displaced towards lower potential values as the pH was increased. Plots of $E_{p,a}$ and $E_{p,c}$ *vs.* pH were linear with slopes of (0.064 ± 0.002) V and (0.064 ± 0.003) V, respectively, indicating clearly that the oxidation/reduction mechanism of OTQ/OTHQ involves the same number of electrons and protons. On the other hand, $E_{p,a}$ and $E_{p,c}$ were practically independent of pH at pH > 8. In addition, the anodic and cathodic currents as well as the anodic and cathodic surface coverage decreased as the pH increased. The surface redox couple response was not observed at pH > 11. Based on these results, 10% ACN + aqueous 1 M $HClO_4$ was chosen as the reaction medium to prepare the adsorbed OTQ, and 1 M $HClO_4$ was chosen for in-depth study on the oxidation/reduction cycle of the adsorbed redox couple.

For these experiments, the working electrode was cycled five times in acidic solution containing the mycotoxin (10% ACN + 90% aqueous 1 M $HClO_4$). Then, the electrode was rinsed with a 1 M $HClO_4$ aqueous solution and transferred to another electrochemical cell which contained only a 1 M $HClO_4$ aqueous solution. Cyclic voltammograms obtained under these experimental conditions at different ν are shown in Fig. 4. A surface-based quasi-reversible redox couple was found, with an anodic peak potential of about 0.64 V. Similar behavior was observed when the electrode was immersed in a solution of OTA, in 10% ACN + 90% aqueous 1 M $HClO_4$, for 60 s under an open circuit and then transferred to another electrochemical cell containing only aqueous 1 M $HClO_4$. During the first anodic scan only one oxidation wave was found in the potential range from 1.2 to 1.4 V. This can be assigned to the oxidation of OTA adsorbed onto the electrode surface. In addition, during the first reverse cathodic scan, only one reduction peak for a surface process was observed, with potential range from 0.75 to 0.55 V, whose complementary anodic peak was found when the second consecutive potential scan was performed (Fig. 5). Successive scans caused an increase in current for this surface quasi-reversible peak system, as well as a decrease of the OTA main oxidation wave. Constant current values were obtained for the surface redox reaction after the third potential scan. Similar

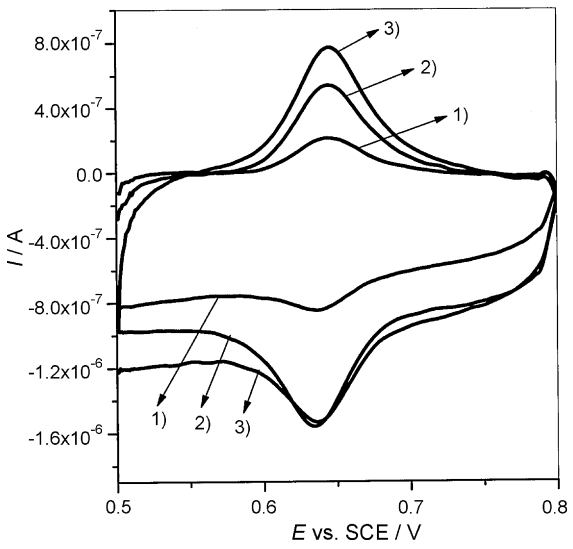

Fig. 4. Cyclic voltammograms of OTHQ obtained in 1 M $HClO_4$ aqueous solution at different scan rates after cycling the working electrode five times in a separate electrochemical cell which contained OTA in 10% ACN + 90% 1 M $HClO_4$ ($c^*_{OTA} = 1.2 \times 10^{-4}$ M). The working electrode was a GC disk of area $A = 0.0707\ cm^2$, and the reference electrode was SCE. ν = (1) 0.010; (2) 0.015 and (3) 0.020 V s^{-1}.

methods were employed to fully characterize the thermodynamics and kinetics of this redox couple using SWV (see below).

The two cathodic peaks as well as the wide anodic peak observed when the consecutive scans were carried out in OTA solutions (Fig. 2) can be assigned to the reduction and oxidation of both OTA by controlled diffusion and adsorbed OTQ/OTHQ, whose reduction and oxidation potentials would be similar (compare Figs. 4 and 5).

The peak shape of OTQ adsorbed onto GC electrodes is independent of scan rate for the range of ν used in this work (0.010–0.050 V s^{-1}). This is theoretically expected for a surface redox couple [27,28]. Repetitive cycling for a minimum of 3 h does not change the voltammograms, demonstrating that this surface redox couple is stable to electrochemical cycling.

The experimental ΔE_p in 1 M $HClO_4$ was (0.007 ± 0.002) V and the average widths at half-height of the anodic and cathodic peaks ($\Delta E_{p/2}$) were (0.051 ± 0.003) V and (0.047 ± 0.002) V, respectively, for the surface quasi-reversible OTHQ/OTQ redox couple (Fig. 4). These results, as well as those previously described for $\partial E_{p,a}/\partial pH$ and $\partial E_{p,c}/\partial pH$ from cyclic voltammograms, indicate quasi-reversible behavior for the adsorbed OTQ/OTHQ redox couple, with an apparent direct $2e^-/2H^+$ exchange in aqueous solution. This is in good agreement with theory when a quinone/hydroquinone-type derivative is responsible for the electroactivity of the compound [29].

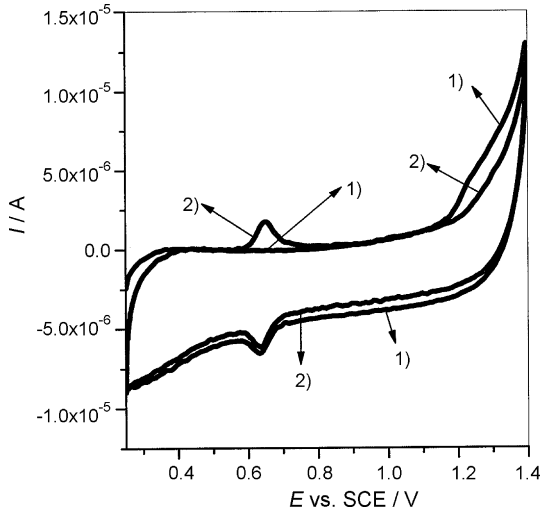

Fig. 5. Consecutive cyclic voltammograms of OTQ/OTHQ recorded in a blank solution of 1 M $HClO_4$, after immersion of the working electrode in a cell containing OTA in 10% ACN + 90% aqueous 1 M $HClO_4$ for 60 s under an open circuit potential. ($c^*_{OTA} = 1.2 \times 10^{-4}$ M), and $\nu = 0.050$ V s^{-1}. (1) and (2) are the first and second scans, respectively.

Where there are no lateral interactions between surface-confined redox centers and a rapid equilibrium is established with the electrode, a zero peak-to-peak splitting (ΔE_p) and a width at half-height of 0.0453 V are expected for a two-electron transfer [27]. Our observation that ΔE_p was simultaneously nonzero and independent of sweep rate, suggests that slow charge transfer kinetics are not the origin of the observed response. Slow kinetics would cause ΔE_p to increase with faster sweep rate. Ohmic effects are also not an explanation for the finite sweep rate independent of ΔE_p because a larger ohmic drop would be expected at higher sweep rates due to the passing of a larger total current. Furthermore, diffusion is effectively excluded as an explanation because the peak current increased linearly with ν, rather than with $\nu^{1/2}$ as expected for diffusion-controlled reactions. There have been previous reports of finite ΔE_p values that are independent of sweep rate for surface-confined redox couples [30]. This unusual quasi-reversibility or apparent non-kinetic hysteresis in cyclic voltammetry has been interpreted in terms of *N*-shaped free energy curves. In this interpretation, unusual hysteretic quasi-reversibility is a non-equilibrium behavior, in which a finite ΔE_p is observed because some rate processes are slow on the time scale of the experiment [31].

The areas under the oxidation and reduction peaks, corrected for any residual charging current, represent charge (Q) associated with the oxidation of OTHQ and the reduction of OTQ, *i.e.*, $Q_{ox} = nFA\Gamma_{OTHQ}$ and $Q_{red} = nFA\Gamma_{OTQ}$, where n is the number of exchanged electrons per mole of oxidized or reduced substance, F is the Faraday constant, A is the microscopic electrode area and Γ_{OTQ} and Γ_{OTHQ} are the surface concentrations of adsorbed oxidized and reduced substance, respectively. Average values of Q_{ox} and Q_{red} of $(2.7 \pm 0.3) \times 10^{-6}$ and $(1.9 \pm 0.2) \times 10^{-6}$ C, respectively, were calculated from cyclic voltammograms recorded with scan rates from 0.015 to 0.100 V s^{-1} when $c^*_{OTA} = 1.2 \times 10^{-4}$ M was employed in the accumulation solution. Further, average values of $(2.0 \pm 0.2) \times 10^{-10}$ and $(1.4 \pm 0.1) \times 10^{-10}$ mol cm^{-2} were obtained for Γ_{OTHQ} and Γ_{OTQ}, respectively, under these experimental conditions. The value obtained for Γ_{OTHQ} represents the saturation surface concentration, $\Gamma_{OTHQ,S}$ (Fig. 6a), *i.e.*, that corresponding to the formation of a monolayer of adsorbed substance (see below). In addition, a tentative expression for Γ_{OTHQ} for a surface redox couple can be expressed as in [27]:

$$\Gamma_{OTHQ} = \left(\frac{4RT}{n^2F^2A}\right)\left(\frac{I_{p,a}}{\nu}\right) \quad (1)$$

An average value of $\Gamma_{OTHQ} = 1.8 \times 10^{-10}$ mol cm^{-2} was obtained from cyclic voltammograms in the 0.010–0.050 V s^{-1} range. This value is in a good agreement with the average value previously determined using the charges of the anodic peaks, as well as with expected values for adsorbed redox couples comprised of similarly sized molecules [27,28,30].

We also examined the isotherms and energetics of adsorption in order to better understand the behavior of this adsorbed redox species. A plot of Γ_{OTHQ} *vs.* c^*_{OTA} is shown in Fig. 6a. The surface concentration rose rapidly with c^*_{OTA} at low c^*_{OTA} and then asymptotically approached the limiting surface concentration. The surface saturation concentration arose at $c^*_{OTA} \geq 1.2 \times 10^{-4} M$. Fits of different adsorption isotherms models (Langmuir, Frumkin, Temkin and Freundlich) were tested to describe the adsorption of OTA anodic

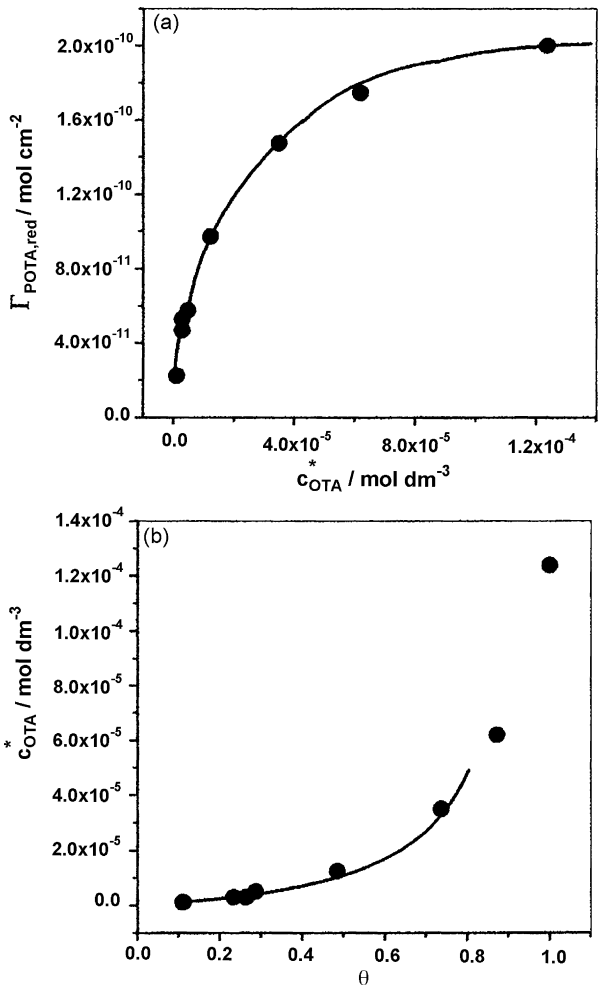

Fig. 6. (a) Surface concentrations of OTHQ *vs.* the OTA bulk concentration. The reaction medium was aqueous 1 M $HClO_4$ and $\nu = 0.050$ V s^{-1}. (b) Experimental data compared with the best-fit Frumkin adsorption isotherm. (●) Indicate experimental points and (–) indicates the best-fit line.

oxidation product at GC electrodes. The best fits were obtained with the Frumkin adsorption isotherm, which is [27]:

$$\beta c^*_{\mathrm{OTA}} = \frac{\theta}{1-\theta}\ \exp(g'\theta) \qquad (2)$$

where $\beta = \exp(-\Delta G_{\mathrm{ads}}/RT)$ is the adsorption coefficient, which expresses the strength of adsorption, $\theta = \Gamma_{\mathrm{OTHQ}}/\Gamma_{\mathrm{OTHQ,S}}$, $g' = 2g\,\Gamma_{\mathrm{OTHQ,S}}/RT$ is a parameter characterizing the interaction between the adsorbed species, and ΔG_{ads} is the Gibbs free energy of adsorption. A plot of c^*_{OTA} against θ is shown in Fig. 6b. The fit was performed for values of $0.1 < \theta < 0.8$ (solid line in Fig. 6b). For the best fit, the parameters were: $\beta = (1.144 \pm 0.004) \times 10^5$, $g' = 0.70 \pm 0.02$ and $\chi^2 = 8.2 \times 10^{-18}$, where χ^2 is the chi-square statistical parameter. There is excellent agreement between experimental data and the results of this fit. A value of $\Delta G_{\mathrm{ads}} = -28.4$ kJ mol^{-1} was obtained for the standard free energy of adsorption. This indicates that the overall adsorption process of OTQ molecules onto the GC surface is energetically favorable. In addition, a positive value for g' indicates that interactions between adsorbed species on the electrode surface are attractive.

3.2. Square wave voltammetry

SW voltammograms are highly sensitive to the charge transfer kinetics of surface redox processes [18,19]. They may be interpreted using two techniques. In the first technique, often called the "quasi-reversible maximum" method, the ratio between the peak current and the frequency is approximated as a parabolic function of the kinetic parameter, κ. In the second technique, the voltammetric peak is split with the SW amplitude at a given frequency [20,21]. According to theory, the maxima of these parabolic functions and the splitting of the voltammetric peak can be used to calculate the formal rate constant, the transfer coefficient and the formal potential of redox couples immobilized on the electrode surface [20–24]. Therefore, a combination of the two techniques is used here to carry out a full characterization of the thermodynamics and kinetics of the OTHQ/OTQ redox couple adsorbed on GC electrodes in 1 M $HClO_4$ aqueous solution.

Forward (I_f), reverse (I_r) and net (I_n) currents were obtained from SW voltammograms of OTHQ adsorbed on GC electrodes after transferring the electrodes to a blank solution (1 M $HClO_4$). Results for the potential region from 0.5 to 0.8 V are shown in Fig. 7 and present strong evidence for the surface-based quasi-reversible nature of this electrochemical signal [29,32].

These findings reveal that the OTA oxidation product selectively interacts with the carbon surface. In principle, this may be explained by the presence of oxygen-containing functional groups, such as carboxylic acid, lactone, o-quinone, p-quinone, carbonyl and phenols, on an activated GC surface [33]. The interaction between these functional groups and the C=O and –COOH groups present in the chemical structure of OTQ (Fig. 1b) might be responsible for the adsorption of this electro-oxidation product onto GC electrodes. Such specific interactions have been previously observed in our laboratory for other mycotoxins [29,32].

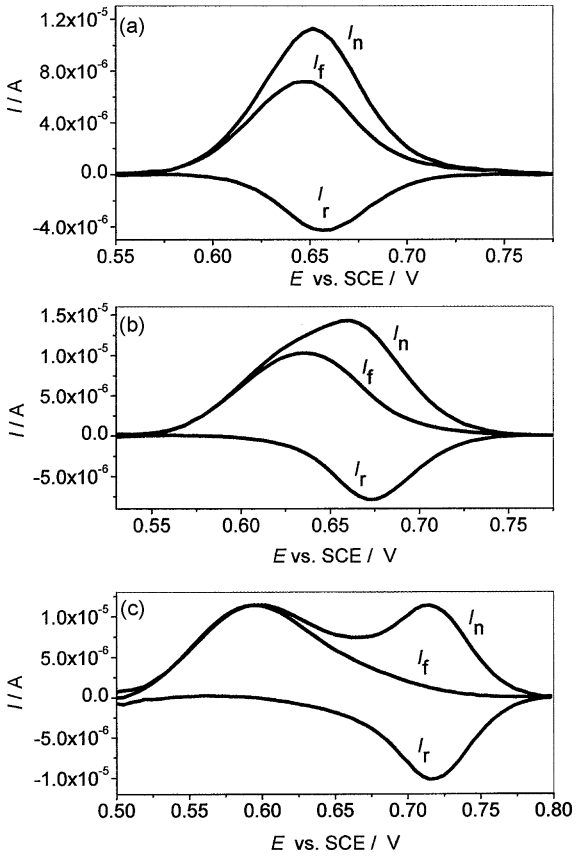

Fig. 7. The forward (I_f), reverse (I_r) and net (I_n) currents from SW voltammograms of OTHQ adsorbed on a GC electrode, recorded in blank solution at different SW amplitudes. ΔE_{SW} were (a) 0.025 V, (b) 0.050 V and (c) 0.100 V. The c^*_{OTA} in the accumulation solution was 1.2×10^{-4} M. The reaction medium was 1 M $HClO_4$ aqueous solution. Other SWV parameters were: $\Delta E_s = 0.005$ V and $f = 10$ Hz.

3.2.1. Determination of thermodynamic and kinetic parameters for OTQ adsorbed at GC electrodes

Plots of $I_{p,n}f^{-1}$ *vs.* f (where $I_{p,n}$ is the net peak current) obtained as previously described after OTQ accumulation onto the GC electrode, are shown in Fig. 8 for two bulk concentrations of mycotoxin.

The apparent reversibility of the confined redox reaction at the electrode surface depends on the kinetic parameter, κ, defined as the ratio between the standard (formal) rate constant (k_s) and the frequency ($\kappa = k_s/f$). Net peak currents from these SW voltammograms are linearly proportional to the frequency, but the factor of this proportionality is a function of the reaction reversibility. If the adsorptions of both the reactant and the product of a quasi-reversible redox couple are equally strong, a maximum appears in the plot of $I_{p,n}f^{-1}$ *vs.* f or f^{-1}, which appears at the SW frequency which is approximately equal to k_s of the redox reaction [19,34]. In the region of the maximum, the curve can be approximated by a parabola, and if $(I_{p,n}f^{-1}) = (I_{p,n}f^{-1})_{max}$, then $f_{max} = k_s/\kappa_{max}$ [34]. Thus, the equation:

$$k_s = \kappa_{max} f_{max} \quad (3)$$

is a convenient way to calculate k_s.

Also, theory predicts that a useful "quasi-reversible maximum" appears only if $-1.5 < \log\delta < 1.5$ [34], where δ is the ratio between the adsorption constants of the oxidized and reduced forms of the surface redox couple.

The theoretically calculated critical kinetics parameter, κ_{max}, depends on the transfer coefficient $(1-\alpha)$, on the product of the SW amplitude and on the number of electrons, $n\Delta E_{SW}$, but it is independent of the normalized potential increment, $n\Delta E_s$ and of the amount of initially adsorbed reactant [34].

In this experiment, the critical frequency, f_{max}, which corresponds to the maximum of an $I_{p,n}f^{-1}$ *vs.* f plot is nearly independent of c^*_{OTA} in the accumulation solution. This behavior suggests that κ_{max} does not depend on the surface coverage. The ratio between peak current and frequency reaches a maximum at $f_{max} = (12 \pm 2)$ Hz.

Theory also predicts that if the rate of reaction becomes rapid, the net peak current of a SW voltammogram splits and the peak height approaches zero [20]. The splitting of the net peak is caused by the skew of forward and reverse peaks on the potential scale, as the dimensionless rate constant increases. Experimentally, this behavior may be observed by decreasing the SW frequency or by increasing the SW amplitude [20]. However, changes in the peak shape, which carry kinetics information, are more effectively produced by varying the SW amplitude rather than varying the frequency [20]. Thus, a set of SWV experiments where c^*_{OTA} and the SW amplitude were varied at a given frequency. The net, forward and reverse currents recorded at a frequency of 10 Hz and at different ΔE_{SW} are shown in Fig. 7. As is theoretically predicted [20,21], large changes in voltammogram shape are obtained when ΔE_{SW} increases for an appropriate fixed frequency. For small ΔE_{SW} (*i.e.*, 25 mV) and $f = 10$ Hz, a single net peak is observed. However, at that frequency the peak starts to split at about $\Delta E_{SW} = 50$ mV and is almost completely split at $\Delta E_{SW} = 100$ mV. The peak splits due to the relationship between the potential-dependent rate constants for the redox couple and the time scale of the experiment. An average value of (0.609 ± 0.003) V for the overall formal potential ($\bar{E}^o_f$) of the adsorbed two-electron redox couple was estimated from the individual potentials. The individual potentials were calculated from the splitting of the anodic and cathodic peaks at frequencies of 10 and 20 Hz (see Table 1), by considering that the two new peaks are symmetrically located about the formal potential of the surface redox couple [20].

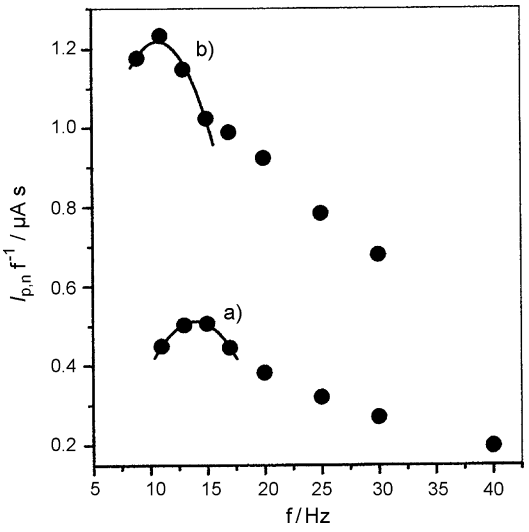

Fig. 8. Dependence of the ratio of net peak current and frequency ($I_{p,n}f^{-1}$) and the SW frequency obtained for OTHQ. The reaction medium was 1 M $HClO_4$ aqueous solution. $\Delta E_{SW} = 0.025$ V and $\Delta E_s = 0.005$ V. The c^*_{OTA} in the accumulation solution was: (a) 1.2×10^{-5} M ($f_{max} = 14\,s^{-1}$) and (b) 1.2×10^{-4} M ($f_{max} = 11\,s^{-1}$). f_{max} was calculated from the first derivative of the mathematical expression for the parabola resulting from a best fit with experimental $I_{p,n}f^{-1}$ values.

It has also been reported that the influence of $(1-\alpha)$ on ΔE_p is insignificant [35]. However, the form of the net SW response for an adsorbed reversible redox couple is influenced by the transfer coefficient [20,35]. For $(1-\alpha) > 0.2$, the ratio between the forward (anodic) and reverse (cathodic) peak currents, $I_{p,a}/I_{p,c}$, can be approximated by a single exponential curve [35]:

$$\left|\frac{I_{p,a}}{I_{p,c}}\right| = 5.6414\ \exp[-3.4606(1-\alpha)] \quad (4)$$

Experimental values for the anodic ($I_{p,a}$) and cathodic ($I_{p,c}$) peak currents, the ratio between $I_{p,a}$ and $I_{p,c}$ and the overall anodic transfer coefficient for the two-electron OTA oxidation product are shown in Table 1. The corresponding average values for these two parameters are $\overline{(I_{p,a}/I_{p,c})} = (1.2 \pm 0.3)$ and $\overline{(1-\alpha)}\,(0.45 \pm 0.06)$, for frequencies of 10 and 20 Hz.

The overall k_s value was calculated through Eq. (3) by using both methods previously mentioned for SW voltammetric analysis. The value $f_{max} = (12 \pm 2)$ Hz was taken from the first method, and κ_{max} was extracted from Table 1 as in Ref. [21] by considering values obtained from the second method, *i.e.*, $n\Delta E_{SW} = 0.050$ mV and $(1-\alpha) = 0.45 \pm 0.06$. Based on these results, Eq. (3) predicts that $\kappa_{max} = 0.89$ and that $k_s = 10.7\,s^{-1}$ for the overall two-electron redox process. These values indicate slower kinetics for this mycotoxin compared with others studied in our laboratory, such as cercosporin ($k_s = 350 \pm 50\,s^{-1}$ and $(1-\alpha) = 0.50 \pm 0.03$ in aqueous 1 M $HClO_4$) [29] and altertoxin-I ($k_s = 685 \pm 27\,s^{-1}$ and $(1-\alpha) = 0.48 \pm 0.03$, in 20% ACN + 1 M $HClO_4$) [32] on the same electrode surface. On the other hand, all transfer coefficients are in the 0.44–0.50 range.

3.2.2. Indirect determination of OTA

Some calibration curves of adsorbed OTA oxidation product generated using SWV are discussed here as a simple introduction for a future publication about the analytical applications of SWV in indirect determination of OTA in real infected matrices. The net current-potential curve in SWV is the most useful analytical signal for this purpose [36]. The high sensitivity of an adsorptive accumulation method is obviously its greatest advantage. The combination of adsorptive accumulation with SWV provides a very valuable electroanalytical tool for performing trace analysis of compounds which are both surface-active and also electroactive. Indirect quantification of OTA was carried out on GC electrodes in unstirred 1 M

Table 1
Anodic ($E_{p,a}$) and cathodic ($E_{p,c}$) peak potentials, anodic ($I_{p,a}$) and cathodic ($I_{p,c}$) peak currents for the split SW peaks, the ratio between $I_{p,a}$ and $I_{p,c}$, $(1-\alpha)$ and $\bar{E}_f^o$ values for the overall two-electron adsorbed redox couple at GC electrodes in 1 M $HClO_4$ aqueous solution generated by the OTA electro-oxidation product (OTQ).

$10^4 c^*_{OTA}$ [a] (mol dm^{-3})	f(Hz)	ΔE_{SW} (V)	$E_{p,a}$ (V)	$I_{p,a}$ (μA)	$E_{p,c}$ (V)	$-I_{p,c}$ (μA)	$I_{p,a}/I_{p,c}$	$(1-\alpha)$
0.12	10	0.050	0.632	3.998	0.676	2.885	1.386	0.41
		0.075	0.617	3.822	0.690	3.065	1.247	0.44
		0.100	0.593	4.296	0.715	3.749	1.146	0.46
		0.125	0.568	3.119	0.739	2.966	1.051	0.48
1.2	10	0.050	0.637	10.285	0.671	7.856	1.309	0.42
		0.075	0.617	9.793	0.695	7.927	1.235	0.44
		0.100	0.593	11.428	0.715	10.204	1.120	0.47
		0.125	0.568	9.643	0.744	9.231	1.045	0.49
1.2	20	0.050	0.642	15.544	0.661	11.233	1.384	0.41
		0.075	0.627	21.504	0.681	18.013	1.194	0.45
		0.100	0.627	21.492	0.681	18.136	1.185	0.45
		0.125	0.588	20.509	0.725	21.261	0.965	0.51

$\overline{(I_{p,a}/I_{p,c})} = (1.2 \pm 0.3)$; $\bar{E}_f^o = (0.609 \pm 0.003)$ V; $\overline{(1-\alpha)} = (0.45 \pm 0.06)$.

[a] c^*_{OTA} is the OTA bulk concentration in the accumulation solution.

$HClO_4$ aqueous solution after cycling the working electrode five times in a solution containing mycotoxin in 10% ACN + 90% 1 M $HClO_4$. Values of $I_{p,n}$ obtained from SW voltammograms recorded at different c^*_{OTA} were used to generate calibration curves. A linear relationship between $I_{p,n}$ and c^*_{OTA} was obtained at f = 10 Hz between 6.2×10^{-8} and 6.0×10^{-6} M. One of the linear regressions obtained by a least square procedure is

$$I_{p,n} = (7.5 \pm 0.3) \times 10^5 c^*_{OTA} - (0.03 \pm 0.05), \quad (r = 0.9943) \qquad (5)$$

$I_{p,n}$ is expressed in μA and c^*_{OTA} has units of mol dm^{-3}. Data used in the regression analysis of each calibration curve are the average of three repeated measurements (10 data points were taken). The percent relative standard deviation (RSD %) calculated from three calibration curves was 4%, and day-to-day reproducibility was 4.9%.

The experimentally determined detection limit (dl) measured experimentally was 1.24×10^{-8} M (5 ppb) with a signal to noise ratio of 3:1. Equivalently, in 10 ml solution, about 50 ng of OTA was indirectly detected. This sensitivity compares favorably with those obtained by other authors using electrochemical techniques. For example, the detection limit was 2.6×10^{-7} M (104 ppb) using SWV in acetate buffer solution with a pH of 4 [17]. The significant (21-fold) improvement in detection limit shows that the highly acidic medium and/or the electrochemical activation of the GC electrode surface makes the adsorption (pre-concentration) of OTQ and its electrochemical discharge much more efficient.

4. Conclusions

We have demonstrated that the OTA electrochemical oxidation product (OTQ) obtained in a highly acidic reaction medium strongly adsorbs at the surface of activated glassy carbon electrodes.

The Frumkin adsorption isotherm best described the specific interaction of OTQ with glassy carbon electrodes. A direct $2e^-/2H^+$ exchange for the redox couple in aqueous solvent could be inferred from the dependence of the electrochemical behavior of adsorbed OTQ on solution pH and from the width at half-height of the anodic and cathodic voltammetric peaks. In addition, a multi-faceted analysis of SWV results enabled full characterization of the thermodynamics and kinetics of the overall two-electron redox couple of the adsorbed species in the highly acidic reaction medium. These results show that SWV is a powerful technique to study redox phenomena of superficial nature.

Moreover, adsorptive accumulation of OTQ appears to be a very promising analytical tool for indirect determination of OTA in real samples.

Acknowledgements

Financial support from Consejo Nacional de Investigaciones Científicas y Técnicas (CONICET), Agencia Nacional de Promoción Científica y Tecnológica (FONCYT) and Secretaría de Ciencia y Técnica (SECyT) from the Universidad Nacional de Río Cuarto is gratefully acknowledged. E.A.R. thanks CONICET and P.A.J.U. thanks MECESUP-CHILE project 0408 for research fellowships.

References

[1] P.S. Steyn, Ochratoxins and related dihydro-isocoumarins, in: V. Bettina (Ed.), Mycotoxins: Production, Isolation, Separation and Purification, Elsevier, New York, 1984, p. 183.
[2] International Agency for Research on Cancer, Some Naturally Occurring Substances: Items and Constituents, Heterocyclic Aromatic Amines and Mycotoxins, Monographs on the Evaluation of Carcinogenic Risk to Humans, vol. 56, IARC, Lyon, France, 1993, p. 489.
[3] N.W. Turner, S. Subrahmanyam, S.A. Piletsky, Anal. Chim. Acta 632 (2009) 168.
[4] P. Krogh, in: P. Krogh (Ed.), Mycotoxins in Food, Academic Press, London, 1987, p. 97.
[5] T. Kuiper-Goodman, P.M. Scott, Biomed. Environ. Sci. 2 (1989) 179.
[6] G.S. Shephard, F. Berthiller, J. Corner, R. Krska, G.A. Lombaert, B. Malone, C. Maragos, M. Sabino, M. Solfrizzo, M.W. Trucksess, H.P. van Egmond, T.B. Whitaker, World Mycotoxin J. 2 (2009) 3.
[7] S. Patel, C.M. Hazel, A.G.M. Winterton, A.E. Gleadle, Food Addit. Contam. 14 (1997) 217.
[8] J.W. Dorner, Chromatographic analysis of mycotoxins, in: T. Shibamoto (Ed.), Chromatographic Analysis of Environmental and Food Toxicants, Marcel Dekker, New York, 1998, p. 113.
[9] M.W. Trucksess, A.E. Poland, Mycotoxin Protocols, Methods in Molecular Biology, vol. 157, Humana Press, Totowa, New Jersey, 2001.
[10] H. Njapau, S. Trujillo, H.P. van Egmond, Mycotoxins and Phycotoxins, Wageningen Academic Publishers, The Netherlands, 2006.
[11] S.H. Alarcón, L. Micheli, G. Palleschi, D. Compagnone, Anal. Lett. 37 (2004) 1545.
[12] S.H. Alarcón, G. Palleschi, D. Compagnone, M. Pascale, A. Visconti, I. Barna-Vetró, Talanta 69 (2006) 1031.
[13] B. Prieto Simón, M. Campás, J.-L. Marty, T. Noguer, Biosens. Bioelectron. 23 (2008) 995.
[14] A.-E. Radi, X. Muñoz-Berbel, M. Cortina Puig, J.-L. Marty, Electrochim. Acta 54 (2009) 2180.
[15] A.-E. Radi, X. Muñoz-Berbel, V. Lates, J.-L. Marty, Biosens. Bioelectron. 24 (2009) 1888.
[16] M.W. Calcutt, I.G. Gillman, R.E. Noftle, R.A. Manderville, Chem. Res. Toxicol. 14 (2001) 1266.
[17] S.C.B. Oliviera, V.C. Diculescu, G. Palleschi, D. Compagnone, A.M. Oliviera Brett, Anal. Chim. Acta 588 (2007) 283.
[18] M. Lovric, S. Komorsky-Lovric, J. Electroanal. Chem. 248 (1988) 239.
[19] S. Komorsky-Lovric, M. Lovric, Fresenius Z. Anal. Chem. 335 (1989) 289.
[20] J.J. OïDea, J.G. Osteryoung, Anal. Chem. 65 (1993) 3090.
[21] S. Komorsky-Lovric, M. Lovric, Electrochim. Acta 40 (1995) 1781.
[22] V. Mirceski, M. Lovric, Electroanalysis 11 (1999) 984.
[23] V. Mirceski, R. Gulaboski, B. Jordanoski, S. Komorski-Lovric, J. Electroanal. Chem. 490 (2000) 37.
[24] F. Garay, V. Solís, J. Electroanal. Chem. 505 (2001) 109.
[25] H. Fernández, M.A. Zón, J. Electroanal. Chem. 322 (1992) 237.
[26] D.M. Anjo, M. Kahr, M.M. Khodabakhsh, S. Nowinski, M. Wanger, Anal. Chem. 61 (1989) 2603.

[27] A.J. Bard, L.R. Faulkner, Electrochemical Methods: Fundamentals and Applications, 2nd ed., Marcel Dekker, New York, 2001.
[28] J. Wang, Analytical Electrochemistry, 3rd ed., Wiley-VCH, USA, 2006.
[29] N.C. Marchiando, M.A. Zón, H. Fernández, Electroanalysis 15 (2003) 40.
[30] R.J. Forster, L.R. Faulkner, J. Am. Chem. Soc. 116 (1994) 5444.
[31] S.W. Feldberg, I. Rubinstein, J. Electroanal. Chem. 240 (1988) 1.
[32] P.G. Molina, M.A. Zón, H. Fernández, Electroanalysis 12 (2000) 791.
[33] R.L. McCreery, Carbon electrodes: structural effects on electron transfer kinetics, in: A.J. Bard (Ed.), Electroanalytical Chemistry, Marcel Dekker, New York, 1991, p. 221.
[34] S. Komorsky-Lovric, M. Lovric, Electrochim. Acta 384 (1995) 115.
[35] V. Mirceski, M. Lovric, Electroanalysis 9 (1997) 1283.
[36] J.O. Osteryoung, J. OïDea, Square wave voltammetry, in: A.J. Bard (Ed.), Electroanalytical Chemistry, Marcel Dekker, New York, 1987, p. 209.